

# Nonclassicality in a cavity quantum optical system

This chapter is based on [12] and is devoted to the investigation of nonclassical features in a physical system comprised of a cavity with two ensembles of two-level atoms has been investigated by considering different configurations of the ensembles with respect to the node and antinode of the cavity field under the framework of open quantum systems. The study reveals the strong presence of nonclassical characters in the physical system by establishing the existence of many facets of nonclassicality, such as the sub-Poissonian Boson statistics and squeezing in single modes, intermodal squeezing, intermodal entanglement, antibunching, and steering. The effect of a number of parameters, characterizing the physical system, on the different aspects of nonclassicality is also investigated. Specifically, it is observed that the depth of the nonclassicality witnessing parameters can be enhanced by externally driving one of the ensembles with an optical field. The work is done in the presence of open system effects, in particular, use is made of Langevin equations along with a suitable perturbative technique.

## 5.1 Introduction

Quantum mechanics has emerged as the best known model of nature, thanks to the spectacular success achieved over the last hundred years. However, only in the last few decades, it is understood that quantum mechanics can even be used to design devices that can outperform their classical counterparts. This quantum power of devices is obtained by exploiting nonclassical states, i.e., states having no classical analogue and more technically, the quantum states having negative values of Glauber-Sudarshan  $P$ -function [2, 131]. Such states are not rare in nature, and entangled and steering states [132], squeezed states [133], antibunched states [134] are typical examples of nonclassical states. The existence of such states were known (at least theoretically) since a long time. In fact, squeezing [135], entanglement [3], and steering [136] were studied even before the pioneering work of Sudarshan [2] that provided a necessary and sufficient criterion of nonclassicality in terms of negativity of  $P$ -function. However, various interesting applications of these nonclassical states were realized only recently with the advent of quantum information processing [137–142] and various facets of atom optics and quantum optics [143, 144]. For example, squeezed vacuum state has been used successfully in detecting gravitational waves in the well known LIGO experiment [145, 146]; squeezed states are also used in continuous variable quantum secure and insecure communication [137, 138]; entanglement is established to be useful in both continuous and discrete variable quantum cryptography [137, 140], and in the realization of schemes for teleportation [141] and dense coding [142]. Additionally, the steerable states provide one-side device independent quantum cryptography [147]. Furthermore, powerful quantum algorithms for unsorted database search [148] to factorization [149], discrete logarithm problem

[149] to machine learning [150] have repeatedly established that quantum computers (which naturally use nonclassical states) can outperform classical computers. In brief, in the last few years, on one hand, we have seen various applications of nonclassical states, and on the other hand, nonclassical features have been reported in a variety of physical systems [151–154], including but not restricted to two-mode Bose-Einstein condensates [153, 155], optical couplers [156, 157], optomechanical [154, 158] and optomechanics-like systems [154, 159], atoms and quantum dot in a cavity [160, 161]. Many of these systems involve different types of cavity which can be produced and manipulated experimentally [162–164]. Naturally, interest in such systems has been considerably enhanced in the recent past. Apart from the applicability of the nonclassical states, and the possibilities of generation and manipulation of these states, another interesting factor that has enhanced the interest on the nonclassical features present in these systems, is the fact that in contrast to the traditional view that quantum mechanics is the science of the microscopic world, these systems having nonclassical properties are often macroscopic [165].

Above facts have provided the motivation for this work which involves the study of nonclassical features of a particular macroscopic system shown in Fig. 5.1. To be specific, we aim to investigate the possibility of observing signatures of various types of nonclassicality in a physical system comprised of a cavity with two ensembles of two-level atoms, placed in different configurations with respect to the Node and Antinode of the cavity field, like, Antinode-Antinode (AA), Antinode-Node (AN), Node-Antinode (NA) and Node-Node (NN). To clearly visualize these configurations, we may note that in AN configuration, one of the ensembles is placed in the Node position of the cavity field and the other one is placed in the Antinode position of the cavity field. Similarly, one can visualize the other configurations studied. Previously, this system was used to study electromagnetically-induced-transparency-like (EIT-like) phenomenon in [323], where an EIT-like phenomenon was observed to appear (disappear) for the NA (AN) configuration. In what follows, we will study the possibilities of observing various types of single mode (e.g., squeezing, sub-Poissonian boson statistics) and intermodal nonclassicality (e.g., intermodal squeezing, antibunching, two and three mode entanglement, steering) in this system by considering that one of the atomic ensembles is driven by an external optical field, and will establish that this external field can be used to control the amount of nonclassicality.

We have already noted that the negativity of  $P$ -function provides us a necessary and sufficient criterion of nonclassicality. However, the  $P$ -function is not always well behaved, and there does not exist any general procedure that can be adapted to experimentally measure it. As a consequence, a set of operational criteria for nonclassicality have been developed over the years. The majority of these nonclassical criteria (in fact, all the criteria used in this work) do not provide any quantitative measure of nonclassicality. Of course, there are some measure of nonclassicality, but each of them have some issues [324], and we have not used any of them in the present study, and they are only sufficient criteria. In fact, there exists an infinite set of nonclassicality criteria involving moments of annihilation and creation operators that are equivalent to the  $P$ -function, but any finite subset of that would be sufficient only. We have used a few such moment-based criteria of nonclassicality [166, 167], each of which is a sufficient criterion only. As none of these criteria provides any quantitative measure of nonclassicality (i.e., as they only provide signatures of nonclassicality), in what follows, these sufficient criteria are frequently referred to as witnesses of nonclassicality. In what follows, through these criteria, different features of nonclassicality are witnessed under the influence of open quantum system evolution.

The effect of the ambient environment is a permanent fixture of nature and needs to be taken into account, especially in experiments related to nonclassical features which are known to be influenced appreciably by the environmental effects. As the present work aims to reveal the nonclassical features present in the system of interest, it would be apt to consider the effect of the environment in our calculations. Such effects are taken into account systematically by using

the framework of open quantum systems [57]. Specifically, decoherence and dissipation are well known open system effects [87] and have been studied on myriad aspects of quantum information, such as in holonomic quantum computation [113], environmental deletion [168], noisy quantum walks [169], quantum cryptography [170] and the effect of squeezing on channel capacity [92]. A precursor of the present theme of nonclassical correlations in the presence of open system effects can be found in [11]. Here, we adapt open system effects on our system of interest by using the formalism of Langevin equations, which is basically the stochastic equations of motion approach [144]. Specifically, the equations of motion for each system mode in the Heisenberg picture are obtained by eliminating the environmental degrees of freedom. The obtained equations of motion for different system modes are usually coupled differential equations and are solved using various perturbative techniques. Here, we have used a perturbative technique that approximates all the higher-order correlations in terms of second-order correlations [171]. The technique has been recently used to study nonclassicality in Raman amplifier [172] and optomechanical oscillator [173].

The rest of the chapter is organized as follows. In Sec. 5.2, we describe the model used in this work in the context of open quantum systems. gives a brief introduction to the various witnesses of nonclassicality used in this work. Subsequently, in Sec. 5.3, we present temporal variation of various witnesses of nonclassicality, introduced in Sec. 2.7.1 of chapter (2), and discuss the significance of the results obtained in this work. Finally, the chapter is concluded in Sec. 5.4.

## 5.2 Cavity containing two ensembles of two-level atoms

The physical system of our interest is briefly described in the previous section and it is schematically shown in Fig. 5.1. In this section, we wish to describe the system in more detail. To begin with, we note that the model physical system of our interest is considered to be made of a single mode cavity ( $\mathcal{S}_{\text{cavity}}$ ) which contains two ensembles ( $\mathcal{S}_A$ —left ensemble and  $\mathcal{S}_B$ —right ensemble) of two level atoms [323]. The left ensemble is driven by a classical optical field having frequency  $\omega_f$ .

The Hamiltonian for the total system  $S \equiv \mathcal{S}_A + \mathcal{S}_B + \mathcal{S}_{\text{cavity}}$ , can be expressed in terms of collective excitation operators  $\hat{A}$  and  $\hat{B}$  in the following form [323]:

$$\hat{H} = \omega_c \hat{C}^\dagger \hat{C} + \omega_a \hat{A}^\dagger \hat{A} + \omega_b \hat{B}^\dagger \hat{B} + \left\{ G_A \hat{C} \hat{A}^\dagger + G_B \hat{C} \hat{B}^\dagger + \chi \hat{A}^\dagger e^{-i\omega_f t} + \text{H.c.} \right\}, \quad (5.1)$$

with

$$\hat{A} = \frac{1}{\sqrt{N_A}} \sum_{i=1}^{N_A} \sigma_{+,A}^i \quad \text{and} \quad \hat{B} = \frac{1}{\sqrt{N_B}} \sum_{j=1}^{N_B} \sigma_{+,B}^j,$$

where H.c., stands for Hermitian conjugate, and  $\sigma_{+,x}^l = |e_x^{(l)}\rangle \langle g_x^{(l)}|$  and  $\sigma_{-,x}^l = |g_x^{(l)}\rangle \langle e_x^{(l)}|$  are the quasispin operators for the  $l$ -th atom in ensemble  $\mathcal{S}_x$  ( $x \in \{A, B\}$ ). The operator  $\hat{C}$  ( $\hat{C}^\dagger$ ) represents the annihilation (creation) operator for the cavity mode. Also,  $G_A = g_A \sqrt{N_A}$ ,  $G_B = g_B \sqrt{N_B}$  and  $\chi = \Omega \sqrt{N_A}$ , where  $g_A$  ( $g_B$ ) is the strength with which the atoms in left (right) ensemble couple with the cavity field. Similarly,  $\Omega$  (or equivalently  $\chi$ ) corresponds to the coupling strength between the atoms in the driven ensemble and the driving field. In the limit of low excitation and large number of atoms ( $N_A$  and  $N_B$ ), the operators  $\hat{A}$  and  $\hat{B}$  satisfy the bosonic commutation relations, i.e.,  $[\hat{A}, \hat{A}^\dagger] \approx [\hat{B}, \hat{B}^\dagger] \approx \mathbf{1}$ , and  $[\hat{A}, \hat{B}] \approx [\hat{A}, \hat{B}^\dagger] \approx 0$ . Therefore, under these conditions,  $\hat{A}$  and  $\hat{B}$

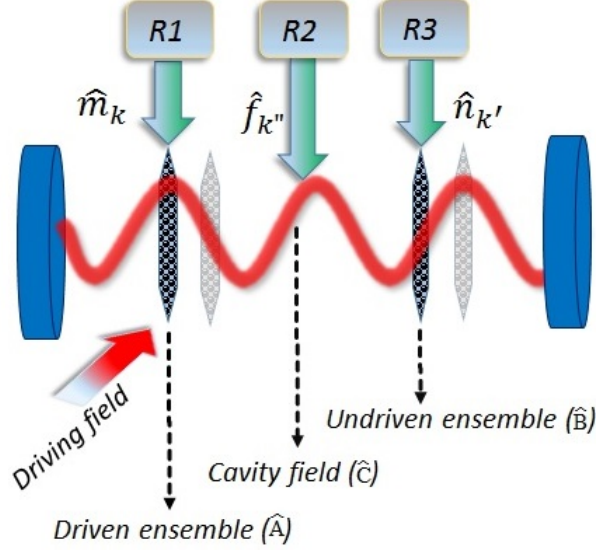


**Figure 5.1:** The schematic representation of the model consisting of a cavity embedded with two ensembles of two-level atoms. The left ensemble  $\mathcal{S}_A$ , with the excitation mode  $\hat{A}$ , is driven by an external field of frequency  $\omega_f$ . The system is studied in configurations: Antinode-Antinode (AA), Antinode-Node (AN), Node-Antinode (NA) and Node-Node (NN). The left ensemble (the driven ensemble), the right ensemble (the undriven ensemble), and the cavity field interact with their independent reservoirs  $R_1$ ,  $R_2$  and  $R_3$  with modes represented by corresponding annihilation operators  $\hat{m}$ ,  $\hat{n}$ , and  $\hat{f}$ , respectively.

can be treated as the annihilation operators for the collective *excitation modes* corresponding to ensembles  $\mathcal{S}_A$  and  $\mathcal{S}_B$ , respectively [323].

In a frame rotating at frequency  $\omega_f$ , governed by the transformation  $\rho \rightarrow S(t)\rho S^\dagger(t)$ , with  $S(t) = \exp[i(\hat{C}^\dagger\hat{C} + \hat{A}^\dagger\hat{A} + \hat{B}^\dagger\hat{B})\omega_f t]$ , the Hamiltonian given by Eq. (5.1) can be expressed in terms of the photonic cavity mode  $\hat{C}$  and the ensemble excitation modes  $\hat{A}$  and  $\hat{B}$ , in the following simplified form [323]

$$\hat{H}_S = \Delta_c \hat{C}^\dagger \hat{C} + \Delta_a \hat{A}^\dagger \hat{A} + \Delta_b \hat{B}^\dagger \hat{B} + \{G_A \hat{C} \hat{A}^\dagger + G_B \hat{C} \hat{B}^\dagger + \chi \hat{A}^\dagger + \text{H.c.}\},$$

where  $\Delta_r = \omega_f - \omega_r$  ( $r \in \{a, b, c\}$ ) represents the frequency detuning of the driven ensemble frequency ( $\omega_a$ ), the un-driven ensemble frequency ( $\omega_b$ ) and the cavity field frequency ( $\omega_c$ ), with respect to the driving frequency  $\omega_f$ .

Open quantum system effects are now taken into consideration by allowing the interaction of the photonic cavity mode  $\hat{C}$  and the collective excitation modes of the ensembles (i.e., modes  $\hat{A}$  and  $\hat{B}$ ) with their respective reservoirs  $R_1$ ,  $R_2$ ,  $R_3$ , Fig. 5.1. This interaction is modeled, under the Markovian white noise approximation, by coupling each mode to a reservoir made up of a collection of harmonic oscillators [57]. As a result, the total Hamiltonian is modified to

$$\hat{H} = \hat{H}_S + \hat{H}_R + \hat{H}_{SR}, \quad (5.2)$$

such that,

$$\hat{H}_R = \sum_k \omega_k \hat{m}_k^\dagger \hat{m}_k + \sum_{k'} \omega_{k'} \hat{n}_{k'}^\dagger \hat{n}_{k'} + \sum_{k''} \omega_{k''} \hat{f}_{k''}^\dagger \hat{f}_{k''}, \quad (5.3)$$

$$\hat{H}_{SR} = \sum_k g_k (\hat{m}_k^\dagger \hat{A} + \hat{A}^\dagger \hat{m}_k) + \sum_{k'} g_{k'} (\hat{n}_{k'}^\dagger \hat{B} + \hat{B}^\dagger \hat{n}_{k'}) + \sum_{k''} g_{k''} (\hat{f}_{k''}^\dagger \hat{C} + \hat{C}^\dagger \hat{f}_{k''}),$$

where  $\hat{m}(\hat{m}^\dagger)$ ,  $\hat{n}(\hat{n}^\dagger)$  and  $\hat{f}(\hat{f}^\dagger)$  are the annihilation (creation) operators corresponding to the reservoirs which interact with and damp the driven ensemble mode  $\hat{A}$ , the un-driven ensemble mode  $\hat{B}$  and the cavity mode  $\hat{C}$ , respectively. Here, and in what follows,  $S$  and  $R$  in the subscript correspond to the system and reservoir, respectively. The resulting (Langevin) equations, for the system operators should include, in addition to the damping terms, the noise operators which would produce fluctuations [144]. We can now explicitly write the Langevin equations for the cavity and atomic ensemble modes. Specifically, the Langevin equations for the cavity mode can be written as

$$\frac{d\hat{C}}{dt} = -i\Delta_c \hat{C} - iG_A \hat{A} - iG_B \hat{B} - \frac{\Gamma_c}{2} \hat{C} + \hat{F}_c, \quad (5.4)$$

where  $\Gamma_c$  is the decay constant and  $\hat{F}_c$  is the noise operator. For the initially uncorrelated subsystems, the initial density matrix can be considered as separable and thus in the tensor product form  $\rho = \rho_S \otimes \rho_R$ , and similarly it may be considered that the expectation value of operator  $M = M_S \otimes M_R$  factors as  $\langle M_S \rangle \langle M_R \rangle$ . Eq. (5.4) is an operator equation and it is not easy to obtain an analytic solution of this type of equations. Keeping this in mind, here we adapt a strategy used in Refs. [171–173]. Following this strategy, we begin our solution scheme by taking an average of each term appearing in this equation with respect to the state  $\rho$ . This step yields a differential equation of the average of  $\hat{C}$  in terms of averages of  $\hat{A}$  and  $\hat{B}$ . Note that this step transforms the operator differential equation into a  $c$ -number differential equation which is much easier to handle. Assuming each reservoir to be in thermal equilibrium at temperature  $T$ , we can average over the system and reservoir degrees of freedom and using the fact that the reservoir average of the noise operator vanishes  $\langle \hat{F}_c \rangle_R = 0$  [144], we end up with the following equation of motion for the average cavity photon number:

$$\frac{d\langle \hat{C} \rangle}{dt} = -i\Delta_c \langle \hat{C} \rangle - iG_A \langle \hat{A} \rangle - iG_B \langle \hat{B} \rangle - \frac{\Gamma_c}{2} \langle \hat{C} \rangle. \quad (5.5)$$

Similarly, we can obtain the Langevin equations for modes  $\hat{A}$  and  $\hat{B}$ , and for all the second order terms in creation and annihilation operators. Averaging each term present in these operator differential equations would lead to a set of coupled ordinary differential equations involving various statistical quantities of interest. In analogy of Eq. (5.5), we obtained Langevin equations for different single and compound modes as follows:

$$\frac{d\langle \hat{A} \rangle}{dt} = -i\Delta_a \langle \hat{A} \rangle - iG_A \langle \hat{C} \rangle - i\chi - \frac{\Gamma_A}{2} \langle \hat{A} \rangle, \quad (5.6)$$

$$\frac{d\langle \hat{B} \rangle}{dt} = -i\Delta_b \langle \hat{B} \rangle - iG_B \langle \hat{C} \rangle - \frac{\Gamma_B}{2} \langle \hat{B} \rangle, \quad (5.7)$$

$$\frac{d\langle \hat{C} \rangle}{dt} = -i\Delta_c \langle \hat{C} \rangle - iG_A \langle \hat{A} \rangle - iG_B \langle \hat{B} \rangle - \frac{\Gamma_c}{2} \langle \hat{C} \rangle, \quad (5.8)$$

$$\frac{d\langle \hat{A}^2 \rangle}{dt} = -2i\Delta_a \langle \hat{A}^2 \rangle - 2iG_A \langle \hat{A} \hat{C} \rangle - 2i\chi \langle \hat{A} \rangle - \Gamma_a \langle \hat{A}^2 \rangle, \quad (5.9)$$

$$\frac{d\langle \hat{B}^2 \rangle}{dt} = -2i\Delta_b \langle \hat{B}^2 \rangle - 2iG_B \langle \hat{B} \hat{C} \rangle - \Gamma_B \langle \hat{B}^2 \rangle, \quad (5.10)$$

$$\frac{d\langle \hat{C}^2 \rangle}{dt} = -2i\Delta_c \langle \hat{C}^2 \rangle - 2iG_A \langle \hat{A} \hat{C} \rangle - 2iG_B \langle \hat{B} \hat{C} \rangle - \Gamma_c \langle \hat{C}^2 \rangle, \quad (5.11)$$

$$\frac{d\langle \hat{A}^\dagger \rangle}{dt} = i\Delta_a \langle \hat{A}^\dagger \rangle + iG_A \langle \hat{C}^\dagger \rangle + i\chi - \frac{\Gamma_A}{2} \langle \hat{A}^\dagger \rangle, \quad (5.12)$$

$$\frac{d\langle \hat{B}^\dagger \rangle}{dt} = i\Delta_b \langle \hat{B}^\dagger \rangle + iG_B \langle \hat{C}^\dagger \rangle - \frac{\Gamma_B}{2} \langle \hat{B}^\dagger \rangle, \quad (5.13)$$

$$\frac{d\langle\hat{C}^\dagger\rangle}{dt} = i\Delta_c\langle\hat{C}^\dagger\rangle + iG_A\langle\hat{A}^\dagger\rangle + iG_B\langle\hat{B}^\dagger\rangle - \frac{\Gamma_c}{2}\langle\hat{C}^\dagger\rangle, \quad (5.14)$$

$$\frac{d\langle(\hat{A}^\dagger)^2\rangle}{dt} = 2i\Delta_a\langle(\hat{A}^\dagger)^2\rangle + 2iG_A\langle\hat{A}^\dagger\hat{C}^\dagger\rangle + 2i\chi\langle\hat{A}^\dagger\rangle - \Gamma_A\langle(\hat{A}^\dagger)^2\rangle, \quad (5.15)$$

$$\frac{d\langle(\hat{B}^\dagger)^2\rangle}{dt} = 2i\Delta_b\langle(\hat{B}^\dagger)^2\rangle + 2iG_B\langle\hat{B}^\dagger\hat{C}^\dagger\rangle - \Gamma_B\langle(\hat{B}^\dagger)^2\rangle, \quad (5.16)$$

$$\frac{d\langle(\hat{C}^\dagger)^2\rangle}{dt} = 2i\Delta_c\langle(\hat{C}^\dagger)^2\rangle + 2iG_A\langle\hat{A}^\dagger\hat{C}^\dagger\rangle + 2iG_B\langle\hat{B}^\dagger\hat{C}^\dagger\rangle - \Gamma_c\langle(\hat{C}^\dagger)^2\rangle, \quad (5.17)$$

$$\frac{d\langle\hat{A}^\dagger\hat{A}\rangle}{dt} = iG_A[\langle\hat{A}\hat{C}^\dagger\rangle - \langle\hat{A}^\dagger\hat{C}\rangle] + i\chi[\langle\hat{A}\rangle - \langle\hat{A}^\dagger\rangle] + \Gamma_A n_A - \Gamma_A\langle\hat{A}^\dagger\hat{A}\rangle, \quad (5.18)$$

$$\frac{d\langle\hat{B}^\dagger\hat{B}\rangle}{dt} = iG_B[\langle\hat{B}\hat{C}^\dagger\rangle - \langle\hat{B}^\dagger\hat{C}\rangle] + \Gamma_B n_B - \Gamma_B\langle\hat{B}^\dagger\hat{B}\rangle, \quad (5.19)$$

$$\frac{d\langle\hat{C}^\dagger\hat{C}\rangle}{dt} = iG_A[\langle\hat{A}^\dagger\hat{C}\rangle - \langle\hat{A}\hat{C}^\dagger\rangle] + iG_B[\langle\hat{B}^\dagger\hat{C}\rangle - \langle\hat{B}\hat{C}^\dagger\rangle] - \Gamma_c\langle\hat{C}^\dagger\hat{C}\rangle + \Gamma_c n_c, \quad (5.20)$$

$$\frac{d\langle\hat{A}\hat{B}\rangle}{dt} = -i(\Delta_a + \Delta_b)\langle\hat{A}\hat{B}\rangle - iG_A\langle\hat{B}\hat{C}\rangle - iG_B\langle\hat{A}\hat{C}\rangle - i\chi\langle\hat{B}\rangle - \frac{\Gamma_A + \Gamma_B}{2}\langle\hat{A}\hat{B}\rangle, \quad (5.21)$$

$$\frac{d\langle\hat{A}\hat{B}^\dagger\rangle}{dt} = i[\Delta_b - \Delta_a]\langle\hat{A}\hat{B}^\dagger\rangle - iG_B\langle\hat{B}^\dagger\hat{C}\rangle + iG_B\langle\hat{A}\hat{C}^\dagger\rangle - i\chi\langle\hat{B}^\dagger\rangle - \frac{\Gamma_A + \Gamma_B}{2}\langle\hat{A}\hat{B}^\dagger\rangle, \quad (5.22)$$

$$\frac{d\langle\hat{A}^\dagger\hat{B}\rangle}{dt} = i(\Delta_a - \Delta_b)\langle\hat{A}^\dagger\hat{B}\rangle + iG_A\langle\hat{B}\hat{C}^\dagger\rangle - iG_B\langle\hat{A}^\dagger\hat{C}\rangle + i\chi\langle\hat{B}\rangle - \frac{\Gamma_A + \Gamma_B}{2}\langle\hat{A}^\dagger\hat{B}\rangle, \quad (5.23)$$

$$\frac{d\langle\hat{A}^\dagger\hat{B}^\dagger\rangle}{dt} = i(\Delta_a + \Delta_b)\langle\hat{A}^\dagger\hat{B}^\dagger\rangle + iG_A\langle\hat{B}^\dagger\hat{C}^\dagger\rangle + iG_B\langle\hat{A}^\dagger\hat{C}^\dagger\rangle + i\chi\langle\hat{B}^\dagger\rangle - \frac{\Gamma_A + \Gamma_B}{2}\langle\hat{A}^\dagger\hat{B}^\dagger\rangle, \quad (5.24)$$

$$\frac{d\langle\hat{B}\hat{C}\rangle}{dt} = -i(\Delta_b + \Delta_c)\langle\hat{B}\hat{C}\rangle - iG_B(\langle\hat{C}^2\rangle + \langle\hat{B}^2\rangle) - iG_A\langle\hat{A}\hat{B}\rangle - \frac{\Gamma_B + \Gamma_c}{2}\langle\hat{B}\hat{C}\rangle, \quad (5.25)$$

$$\frac{d\langle\hat{B}\hat{C}^\dagger\rangle}{dt} = -i(\Delta_b - \Delta_c)\langle\hat{B}\hat{C}^\dagger\rangle + iG_B(\langle\hat{B}^\dagger\hat{B}\rangle - \langle\hat{C}^\dagger\hat{C}\rangle) + iG_A\langle\hat{A}^\dagger\hat{B}\rangle - \frac{\Gamma_B + \Gamma_c}{2}\langle\hat{B}\hat{C}^\dagger\rangle, \quad (5.26)$$

$$\frac{d\langle\hat{B}^\dagger\hat{C}\rangle}{dt} = i(\Delta_b - \Delta_c)\langle\hat{B}^\dagger\hat{C}\rangle + iG_B[\langle\hat{C}^\dagger\hat{C}\rangle - \langle\hat{B}^\dagger\hat{B}\rangle] - iG_A\langle\hat{A}\hat{B}^\dagger\rangle - \frac{\Gamma_B + \Gamma_c}{2}\langle\hat{B}^\dagger\hat{C}\rangle, \quad (5.27)$$

$$\frac{d\langle\hat{B}^\dagger\hat{C}^\dagger\rangle}{dt} = -i(\Delta_b + \Delta_c)\langle\hat{B}^\dagger\hat{C}^\dagger\rangle + iG_B[\langle(\hat{C}^\dagger)^2\rangle + \langle(\hat{B}^\dagger)^2\rangle] + iG_A\langle\hat{A}^\dagger\hat{B}^\dagger\rangle - \frac{\Gamma_B + \Gamma_c}{2}\langle\hat{B}^\dagger\hat{C}^\dagger\rangle, \quad (5.28)$$

$$\frac{d\langle\hat{A}\hat{C}\rangle}{dt} = -i(\Delta_a + \Delta_c)\langle\hat{A}\hat{C}\rangle - iG_A[\langle\hat{C}^2\rangle + \langle\hat{A}^2\rangle] - iG_B\langle\hat{A}\hat{B}\rangle - i\chi\langle\hat{C}\rangle - \frac{\Gamma_A + \Gamma_c}{2}\langle\hat{A}\hat{C}\rangle, \quad (5.29)$$

$$\frac{d\langle\hat{A}\hat{C}^\dagger\rangle}{dt} = i(\Delta_c - \Delta_a)\langle\hat{A}\hat{C}^\dagger\rangle + iG_A[\langle\hat{A}^\dagger\hat{A}\rangle - \langle\hat{C}^\dagger\hat{C}\rangle] + iG_B\langle\hat{A}\hat{B}^\dagger\rangle - i\chi\langle\hat{C}^\dagger\rangle - \frac{\Gamma_A + \Gamma_c}{2}\langle\hat{A}\hat{C}^\dagger\rangle, \quad (5.30)$$

$$\frac{d\langle\hat{A}^\dagger\hat{C}\rangle}{dt} = i(\Delta_a - \Delta_c)\langle\hat{A}^\dagger\hat{C}\rangle + iG_A[\langle\hat{C}^\dagger\hat{C}\rangle - \langle\hat{A}^\dagger\hat{A}\rangle] - iG_B\langle\hat{A}^\dagger\hat{B}\rangle + i\chi\langle\hat{C}\rangle - \frac{\Gamma_A + \Gamma_c}{2}\langle\hat{A}^\dagger\hat{C}\rangle, \quad (5.31)$$

$$\frac{d\langle\hat{A}^\dagger\hat{C}^\dagger\rangle}{dt} = i(\Delta_a + \Delta_c)\langle\hat{A}^\dagger\hat{C}^\dagger\rangle + iG_A[\langle(\hat{C}^\dagger)^2\rangle + \langle(\hat{A}^\dagger)^2\rangle] + iG_B\langle\hat{A}^\dagger\hat{B}^\dagger\rangle - \frac{\Gamma_A + \Gamma_c}{2}\langle\hat{A}^\dagger\hat{C}^\dagger\rangle. \quad (5.32)$$

Here,  $n_A$ ,  $n_B$  and  $n_C$  represent the thermal photon numbers corresponding to mode  $A$ ,  $B$  and  $C$ , respectively. Also, it would be apt to note that one can express the various witnesses of nonclassicality described in Sec. 2.7.1 in terms of the solutions of the above set of coupled differential equations, which can be obtained using Mathematica or similar programs or by using conventional methods of obtaining analytic solutions of the coupled differential equations. Particularly, in this work, we have used Mathematica to obtain simultaneous numerical solution of these coupled differential equations.

To illustrate the method adapted in this work to obtain the expressions for nonclassicality witnesses using the solution of the above equations, we may consider the computation of Mandel parameter as an example. Mandel parameter defined by Eq. (5.3) contains the term  $\langle(\hat{A}^\dagger\hat{A})^2\rangle$ . This quantity is not among the variables appearing in the above equations. So the solution of the above set of coupled equations would not provide us an expression for  $\langle(\hat{A}^\dagger\hat{A})^2\rangle$ . To circumvent this problem, we have adapted a technique that allows us to simplify this term after writing it in normal-ordered form  $\langle(\hat{A}^\dagger\hat{A})^2\rangle = \langle\hat{A}^\dagger\hat{A}^\dagger\hat{A}\hat{A}\rangle + \langle\hat{A}^\dagger\hat{A}\rangle$  and subsequently using the decoupling relation [171]  $\langle ABCD\rangle \approx \langle AB\rangle\langle CD\rangle + \langle AC\rangle\langle BD\rangle + \langle AD\rangle\langle BC\rangle - 2\langle A\rangle\langle B\rangle\langle C\rangle\langle D\rangle$ . Using this decoupling relation we can write

$$\begin{aligned}\langle\hat{A}^\dagger\hat{A}^\dagger\hat{A}\hat{A}\rangle &\approx \langle\hat{A}^\dagger\hat{A}^\dagger\rangle\langle\hat{A}\hat{A}\rangle + \langle\hat{A}^\dagger\hat{A}\rangle\langle\hat{A}^\dagger\hat{A}\rangle + \langle\hat{A}^\dagger\hat{A}\rangle\langle\hat{A}^\dagger\hat{A}\rangle - 2\langle\hat{A}^\dagger\rangle\langle\hat{A}^\dagger\rangle\langle\hat{A}\rangle\langle\hat{A}\rangle, \\ &= \langle(\hat{A}^\dagger)^2\rangle\langle\hat{A}^2\rangle + 2\langle\hat{A}^\dagger\hat{A}\rangle^2 - 2\langle\hat{A}^\dagger\rangle^2\langle\hat{A}\rangle^2.\end{aligned}\quad (5.33)$$

Interestingly, the Mandel parameter can now be expressed in terms of the variables, time evolution of which is obtained as the solution of the above set of differential equation and we can express Mandel parameter (2.41) as

$$Q_M \approx \frac{\langle(\hat{A}^\dagger)^2\rangle\langle\hat{A}^2\rangle + \langle\hat{A}^\dagger\hat{A}\rangle^2 - 2\langle\hat{A}^\dagger\rangle^2\langle\hat{A}\rangle^2}{\langle\hat{A}^\dagger\hat{A}\rangle}.\quad (5.34)$$

Clearly, the solution of the coupled differential equation listed above would now allow us to study the temporal evolution of the Mandel parameter and thus to investigate the presence of nonclassicality in our system of interest under the framework of open quantum system. Similar strategy is adapted in the study of all other witnesses of nonclassicality mentioned above and this is how the interesting results related to the temporal evolution of nonclassicality witnesses illustrated in Figs. 5.3-5.11, and summarized in Table 5.1, are obtained.

In general, these coupled differential equations are required to be decoupled using an appropriate approximation scheme. Now, we may move to the next section, where we study various measurable criteria of nonclassicality, discussed in Sec. 2.7.1 of chapter 2, to investigate the presence of nonclassicality in the physical system of our interest.

### 5.3 Results and Discussion

In this section, we study the nonclassical properties of our system. The analysis is carried out by placing the ensembles in the four configurations, viz., AA, AN, NA, and NN configurations. The investigation performed for all the configurations is summarized in Table 5.1. It clearly emerges that the AA configuration is more suited for observing the various facets of nonclassicality in the system. In some cases, other configurations may be preferred due to sufficient depth of the nonclassicality witness, which is desired in some particular applications having practical relevance. The effect of external driving field on the various nonclassical witnesses is studied with respect to  $\Delta t$ , where  $\Delta$  is the common detuning for the three modes  $\hat{A}$ ,  $\hat{B}$  and  $\hat{C}$ . The various parameters used for AN configuration are  $G_A = 0.2\Delta$ ,  $G_B = 0.02\Delta$ ,  $\Gamma_A = 2\Delta$ ,  $\Gamma_B = 0.2\Delta$ ,

and  $\Gamma_C = 0.2\Delta$ . For NA configuration,  $G_A = 0.02\Delta$ ,  $G_B = 0.2\Delta$ ,  $\Gamma_A = 0.2\Delta$ ,  $\Gamma_B = 2\Delta$ , and  $\Gamma_C = 0.2\Delta$ . For AA configuration,  $G_A = 0.2\Delta$ ,  $G_B = 0.2\Delta$ ,  $\Gamma_A = 2\Delta$ ,  $\Gamma_B = 2\Delta$ , and  $\Gamma_C = 0.2\Delta$ . And finally, for NN configuration  $G_A = 0.02\Delta$ ,  $G_B = 0.02\Delta$ ,  $\Gamma_A = 0.2\Delta$ ,  $\Gamma_B = 0.2\Delta$ , and  $\Gamma_C = 0.2\Delta$ . In all the cases, we have considered here vacuum bath.

The initial conditions (at  $t = 0$ ) are chosen in such a way that the average number of photons in the cavity field and the average number of excitations in the two ensembles are all equal to 1. Figure 5.2 shows the evolution of the average number of bosons corresponding to the driven ensemble mode ( $\langle \hat{A}^\dagger \hat{A} \rangle$ ), the undriven ensemble mode ( $\langle \hat{B}^\dagger \hat{B} \rangle$ ) and the average number of the cavity photons ( $\langle \hat{C}^\dagger \hat{C} \rangle$ ). The average number of excitations is found to drop quickly for the ensemble placed at the Antinode of the cavity field, compared to the ensemble placed at the Node of the cavity field. One can also see vivid variations in the average excitation number of the driven ensemble, when placed at the Node of the cavity field. In other words, placing the ensemble at the Antinode of the cavity field, shadows the effect of the external field. We have not shown similar variation in the boson number for remaining two configurations as it is quite similar to what is observed here.

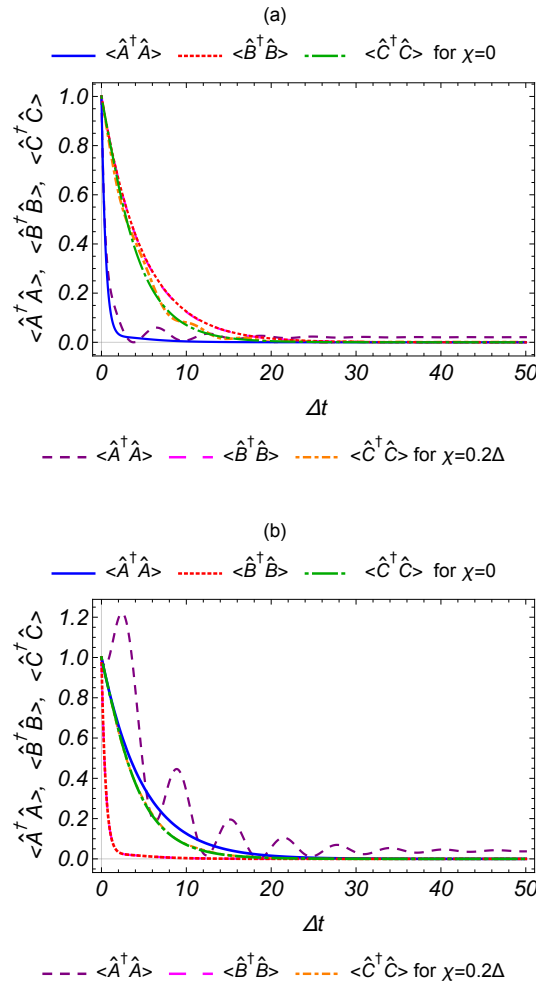


**Figure 5.2:** Average number of cavity photons and excitations corresponding to the two ensembles, studied with respect to the dimensionless parameter  $\Delta t$ . (a) and (b) correspond to AN (left ensemble at Antinode and the right ensemble at Node) and NA (left ensemble at Node and the right ensemble at Antinode) configurations, respectively. The average number of excitations corresponding to the driven ensemble ( $\langle \hat{A}^\dagger \hat{A} \rangle$ ), the undriven ensemble ( $\langle \hat{B}^\dagger \hat{B} \rangle$ ) and the average cavity photon number ( $\langle \hat{C}^\dagger \hat{C} \rangle$ ) is depicted for  $\chi = 0$  and  $\chi = 0.2\Delta$ . All the quantities shown in the plots are dimensionless.



Evolution of the average boson number discussed above gives us a feeling of the system dynamics, but does not provide us any information about the nonclassical nature of the system. To obtain the nonclassical characteristics of the system, we begin with the study of variation of a single mode nonclassicality witness known as Mandel parameter  $Q_M$ , defined in Eq. (5.2). Variation of  $Q_M$  with respect to rescaled time  $\Delta t$  is plotted in Fig. 5.3 for all three modes of the system in AN and NA configurations. The condition for nonclassicality is implied by the negative values of  $Q_M$  (i.e.,  $Q_M < 0$ ) and can be interpreted as the sub-Poissonian statistics of the corresponding field. Further, it is observed that the application of the external field to the driven ensemble makes  $Q_M$  more negative, and thus the driving optical field may be used to enhance the amplitude of the nonclassicality witness in both the driven ensemble and cavity mode. Negative values of  $Q_M$  are also observed for AA and NN configurations and similar inferences can be drawn from it as mentioned in Table 5.1. Specifically, we found nonclassicality in the driven (undriven) ensemble in the absence of the external drive. Although in the absence of the driving term, the Hamiltonian given by Eq. (5.1) is symmetric for both the ensembles, the observed behavior can be attributed to different values of decay constants for the modes under consideration. Note that the nonclassicality observed in the driven ensemble for higher intensity of the driving field establishes that driving field can be used to control the amount of nonclassicality in the system.

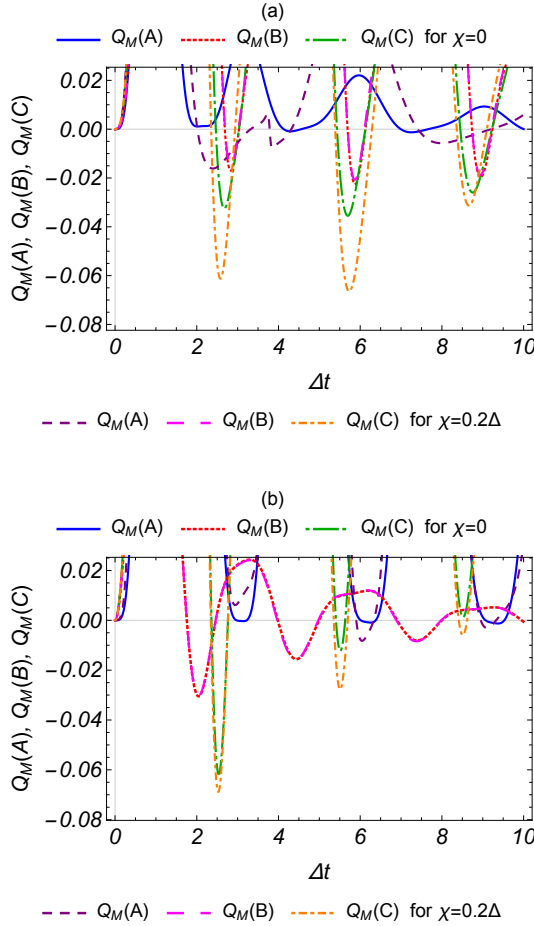


**Figure 5.3:** Mandel parameter with respect to the dimensionless parameter  $\Delta t$ . Figures (a) and (b) correspond to AN and NA configurations, respectively. The nonclassical nature of the field corresponding to the mode  $\alpha$  is confirmed by  $Q_M(\alpha) < 0$ .

Motivated by the presence of single mode nonclassicality in the boson number distribution also illustrating the presence of single mode antibunching, we also study the possibilities of compound mode antibunching using Eq. (2.45). Fig. 5.4 shows the variation of nonclassicality param-

eter for the intermodal antibunching as defined by Eq. (2.45) for all possible compound modes in AN and NA configuration. The criterion  $\mathcal{A}_{\alpha\beta} < 0$  is satisfied for all the modes  $\alpha/\beta \in \{\hat{A}, \hat{B}, \hat{C}\}$ . One can see the enhancement in the depth of intermodal antibunching parameter by the action of the external field driving the ensemble  $A$ . Similar studies in the case of AA and NN configurations also show intermodal antibunching as summarized in Table 5.1.

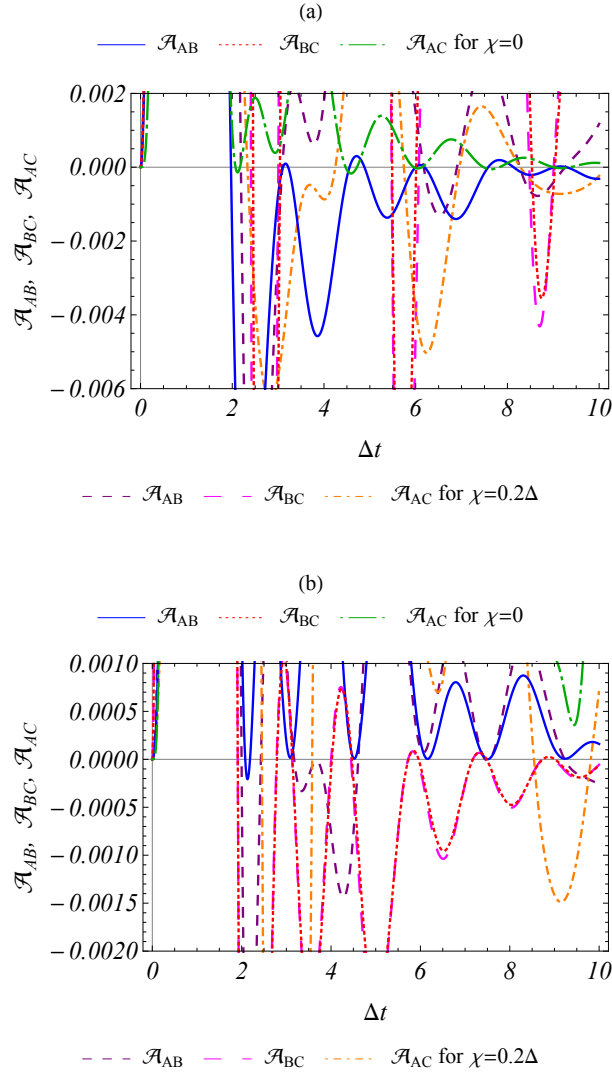


**Figure 5.4:** Showing intermodal antibunching parameter  $\mathcal{A}_{\alpha\beta}$  for modes  $\alpha$  and  $\beta$ , plotted with respect to the parameter  $\Delta t$ . (a) and (b) correspond to AN and NA configurations, respectively. The existence of intermodal antibunching is confirmed if  $\mathcal{A}_{\alpha\beta} < 0$ .

After witnessing the signatures of nonclassicality in all three modes of the system through the negative values of the Mandel  $Q_M$  parameter, we turn our attention towards single mode squeezing; criterion for which is defined in Eq. (2.47) and Eq. (2.48). Fig. 5.5 illustrates the presence of the quadrature squeezing in all the individual modes, both in AN and NA configurations. A similar study for AA and NN configurations is carried out and the results (not displayed here) are summarized in Table 5.1. The field mode  $\hat{A}$ , corresponding to the driven ensemble, shows an appreciable enhancement in the magnitude of squeezing illustrated by the decrease of the variance in one quadrature with respect to the coherent state level as soon as the external field is applied. This enhancement is also observed in the undriven mode  $\hat{B}$  and the cavity mode  $\hat{C}$ , but with relatively lesser magnitude in AN configuration, while as in NA configuration, the enhancement in the nonclassicality of field modes  $\hat{B}$  and  $\hat{C}$  is quite meager. This can be attributed to the fact that in

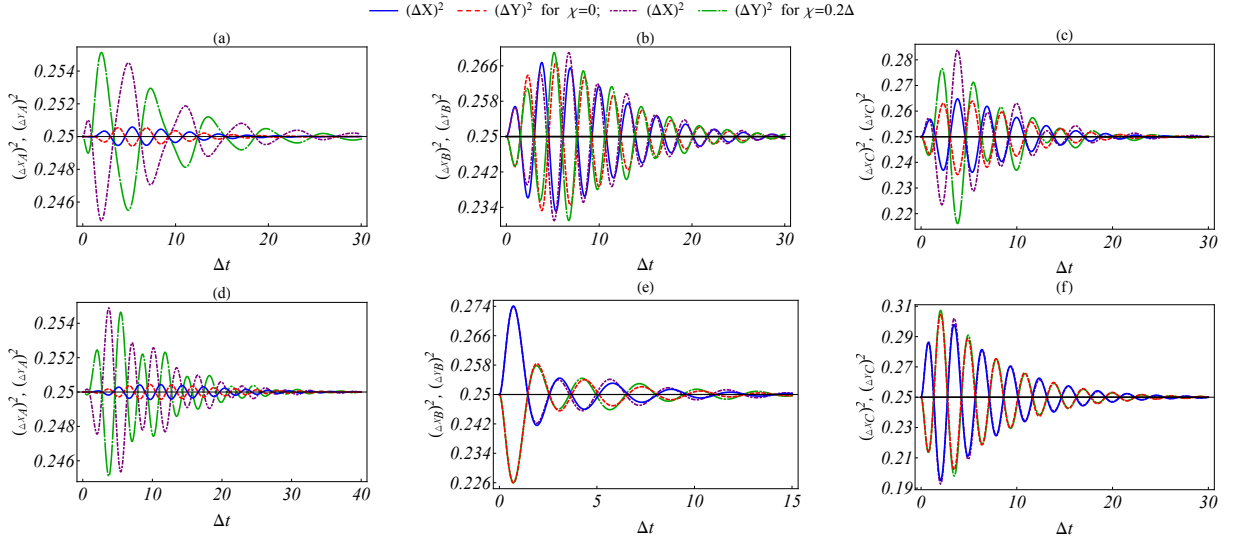


**Figure 5.5:** Single mode squeezing, as defined in Eqs. (2.47) and (2.48), plotted with respect to the dimensionless parameter  $\Delta t$ . Sub-figures (a)-(d), (b)-(e) and (c)-(f) correspond to modes  $\hat{A}$ ,  $\hat{B}$  and  $\hat{C}$ , respectively. The top and bottom panels pertain to the AN and NA configurations, respectively. It is clear that the application of the external field to the driven ensemble ( $\hat{A}$ ), that is, the non-zero value of  $\chi$ , enhances the squeezing in the respective quadratures of a particular mode.

NA configuration, the driven ensemble, being at the node of the cavity field, is weakly coupled to it. Therefore, we conclude that the amount of nonclassicality in the driven ensemble can be controlled by the strength of the driving field, however, the driven ensemble should be placed at the Antinode of the cavity field (AN or AA configurations) for this control to be effective on the cavity field mode ( $\hat{C}$ ) and the undriven ensemble excitation mode ( $\hat{B}$ ), as well. However, in some cases (as in Fig. 5.5 (b)), with an increase in the strength of the external field nonclassicality present in the absence of external field decreases initially for a small period of time before increasing thereafter. This behavior could not be explained by the present study and may be attempted in the near future. The role of external driving field strength as a control parameter can be further established using Fig. 5.6, which illustrates the variation of  $(\Delta X_a)^2$  with respect to the external driving field strength and time. The enhancing effect of the external field on the quadrature squeezing is clearly visible in this case.

Motivated by the observation for the single mode squeezing, we investigate the presence of intermodal squeezing using the criterion given in Eqs. (2.49a) and (2.49b). The outcome of the investigation is plotted in Fig. 5.7, which clearly shows the existence of intermodal squeezing in the compound mode  $\hat{A}\hat{B}$ . One can observe the amplification in the squeezing parameters as a consequence of an increase in the external field driving the atomic ensemble  $\mathcal{S}_A$  (cf. Fig. 5.7 (b)). A similar study for NN and AA configuration is also carried out with compound modes  $\hat{B}\hat{C}$  and  $\hat{A}\hat{C}$  in all four configurations. The presence of squeezing in different possible compound ensemble-ensemble and ensemble-cavity modes in all the four configurations is observed and is summarized in Table 5.1. It is worth mentioning here that the enhancement in the values of the witness of the intermodal squeezing is found to be more prominent in the compound mode  $\hat{A}\hat{C}$  when compared with  $\hat{A}\hat{B}$  or  $\hat{B}\hat{C}$ . This can be attributed to the fact that the amount of nonclassicality in mode  $\hat{B}$  is less susceptible to the driving field.

Nonclassical features manifested through the negative values of Mandel  $Q_M$  parameter, intermodal antibunching and the criteria of single mode and compound mode squeezing have been studied since long using various techniques including short-time approach [325, 326] and Sen-

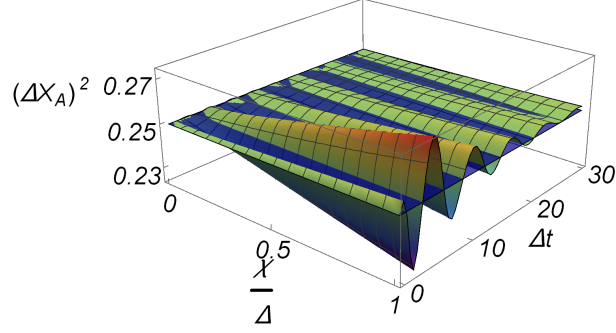


**Figure 5.6:** Showing squeezing parameter  $(\Delta X_A)^2$  for mode  $\hat{A}$  as a function of the driving field strength  $\chi$  as well as the dimensionless parameter  $\Delta t$ . The enhancing effect in quadrature squeezing as a result of increase in the strength of the driving field is observed.

Mandal approach [156, 327], but most of those studies were limited to closed system configuration. In the present work, we have reported the existence and dynamics of these nonclassical features in the backdrop of open quantum systems. To continue the investigation further, we may note that among various nonclassical features, entanglement has drawn maximum attention of the scientific community because of its enormous applications in quantum computing and communication and because of the fact that it may lead to various phenomenon having no classical analogue such as, dense coding [142] and teleportation [141]. Keeping this in mind, we would now look into the possibility of observing intermodal entanglement in the system of our interest. To do so, we will use a set of inseparability criteria, each of which is only sufficient and consequently when one of the criteria fails, another one may succeed to detect entanglement. We begin with Duan's criterion for inseparability defined in Eq. (2.50) and graphically present the obtained results in Fig. 5.8. It is clear from Fig. 5.8 that the condition for inseparability (i.e.,  $\mathcal{D}_{\alpha\beta} < 0$ ) is satisfied for modes  $\alpha$  and  $\beta$ . Irrespective of whether the driven ensemble is placed at Node or Antinode of the cavity field, the value of the Duan parameters  $\mathcal{D}_{AB}$  and  $\mathcal{D}_{BC}$  is very small. In the NA configuration (shown in Fig. 5.8 (b)), the Duan parameter  $\mathcal{D}_{AB}$ ,  $\mathcal{D}_{BC}$  as well as  $\mathcal{D}_{AC}$  become negative, thereby witnessing the presence of entanglement among all the modes. On the other hand, in AN configuration,  $\mathcal{D}_{BC}$  is non-negative (cf. Fig. 5.8 (a)). This implies that transforming the system from AN to NA configuration enhances the intermodal entanglement, which can also be viewed in the enhancement of the Duan parameter  $\mathcal{D}_{AC}$  in NA configuration.

As stated above, moment-based criteria of inseparability are only sufficient. Hence, it makes sense to look into the possibility of observing entanglement in light of one or more different criteria. We study the famous Hillery-Zubairy criteria defined by Eqs. (2.51) and (2.52) and have illustrated the corresponding results in Fig. 5.9, where negative values of the parameters  $\mathcal{E}_{AB}$  and  $\tilde{\mathcal{E}}_{AB}$  confirm the existence of the intermodal entanglement between modes  $\hat{A}$  and  $\hat{B}$  for all configurations. At times, weak signatures of entanglement are found through  $\tilde{\mathcal{E}}_{AB}$  criterion, but relatively stronger signatures are found through  $\mathcal{E}_{AB}$  criterion (see Fig. 5.9). Similarly, one may observe in Fig. 5.8-(a) and 5.9-(b) that, at  $\Delta t = 6$ , Duan's criterion failed to detect entanglement but is captured by the Hillery-Zubairy criteria. Further, the study revealed the relevance of placement of ensembles in the cavity for the generation of entanglement between two spatially separated ensembles interacting with a common cavity field. Also, going from AA to NN configuration, the effect of external driving field becomes relevant for controlling the amount of entanglement. A similar study for the remaining two compound modes  $\hat{B}\hat{C}$  and  $\hat{A}\hat{C}$  also established that they are always entangled in all configurations as summarized in Table 5.1.

As we have already mentioned, entangled states may or may not satisfy steering condition, but a state satisfying steering condition must be entangled. Thus, a steering criterion can be viewed

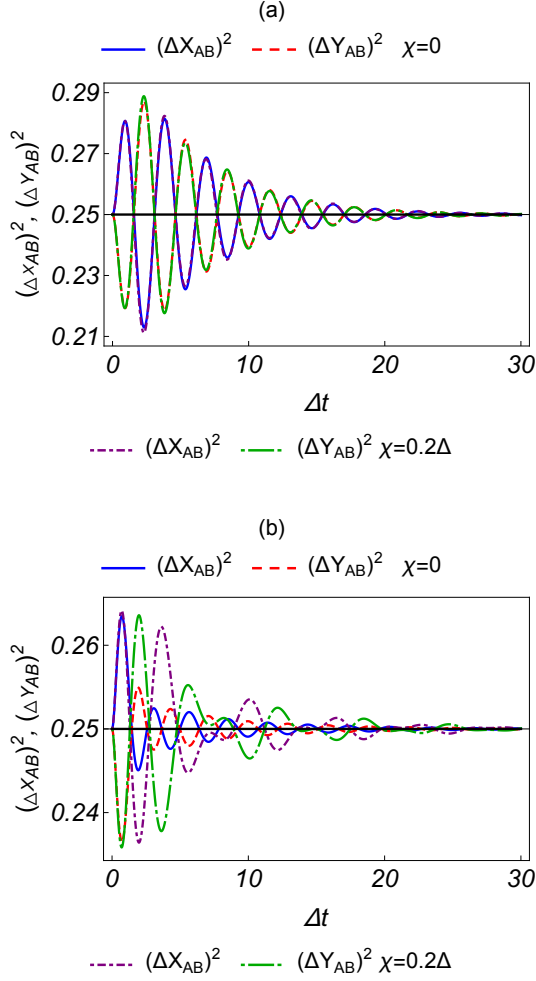


**Figure 5.7:** Showing inter-modal squeezing, defined by Eq. (2.49a), with respect to  $\Delta t$ . (a) and (b) show the squeezing in compound mode  $\hat{A}\hat{B}$ , in AN and NA configurations, respectively. One finds enhancement in the intermodal squeezing as a result of driving ensemble ( $\hat{A}$ ) by the application of the external field.

as a stronger criterion of nonclassicality in comparison to the criteria of entanglement. Further, entangled states that are not steered cannot be used for one-way device independent quantum cryptography, but steered states can be [147]. This motivated us to look into the possibility of observing steered states in our system. To do so we have used the steering criterion given by Eq. (2.54) and plotted, for example, for two spatially separated ensembles modes  $\hat{A}$  and  $\hat{B}$  in Fig. 5.10. The existence of the steered state is observed for modes  $\hat{A}$  and  $\hat{B}$  (also for  $\hat{B}$  and  $\hat{C}$  and for  $\hat{A}$  and  $\hat{C}$  as summarized in Table 5.1) for all configurations. Further, in contrast to entanglement witnesses, here we observe an asymmetric nature of steering which is reflected from Fig. 5.10, where it can be seen that  $\mathcal{S}_{AB} \neq \mathcal{S}_{BA}$ . For instance, Fig. 5.10-c shows that for non-zero driving field intensity,  $\hat{A}$  can steer  $\hat{B}$ , while the converse is not observed. The results obtained for the steering criterion established the same observations as found for the Hillery Zubairy entanglement criteria. Failure to obtain steering in some of the cases (as highlighted in Table 5.1) establishes that it is a relatively stronger criterion of nonclassicality, and the presence of steering correlations in two spatially separated ensembles, mediated by the cavity field and controllable by the external driving, is an interesting observation.

So far we have seen quantum correlations involving two modes only. However, our system

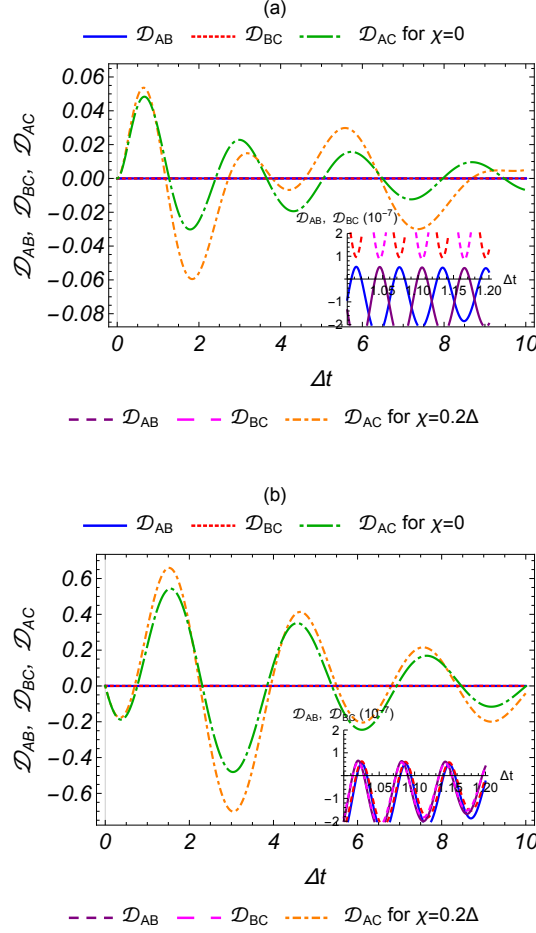


**Figure 5.8:** Showing Duan separability parameter against  $\Delta t$ . Figures (a) and (b) correspond to AN and NA configurations, respectively. The sufficient condition for inseparability is implied by  $\mathcal{D}_{\alpha\beta} < 0$ , for modes  $\alpha$  and  $\beta$ .

consists of three modes that are treated quantum mechanically. Hence, we may extend our study to check nonclassical features of the system through some quantum correlations involving all the three modes  $\hat{A}$ ,  $\hat{B}$  and  $\hat{C}$ . To do so, use has been made of the biseparability criteria defined in Eqs. (2.55) and (2.56), to study multimode entanglement. Corresponding results are plotted in Fig. 5.11. It is clear that the sufficient condition for the fully entangled state, which is the satisfaction of at least one of the two sets of inequalities given by (2.57) and (2.58), is satisfied here. Thus, there exists a nonclassical correlation involving all the three modes in both AN and NA configuration. Specifically, all possible combinations for the biseparability show almost similar variation in Fig. 5.11. This establishes that the three-mode compound state is fully entangled. The application of the external field is found to enhance the signature for the existence of the multimode entanglement. Similar study for other configurations is summarized in Table 5.1.

## 5.4 Conclusion

In the previous sections, we have performed a detailed investigation on the temporal variation of various witnesses of nonclassicality present in a model physical system consisting of a cavity that contains two ensembles of two level atoms which are placed in different configurations with respect to the Antinode and Node of the cavity field, viz., AA, AN, NA and NN configura-

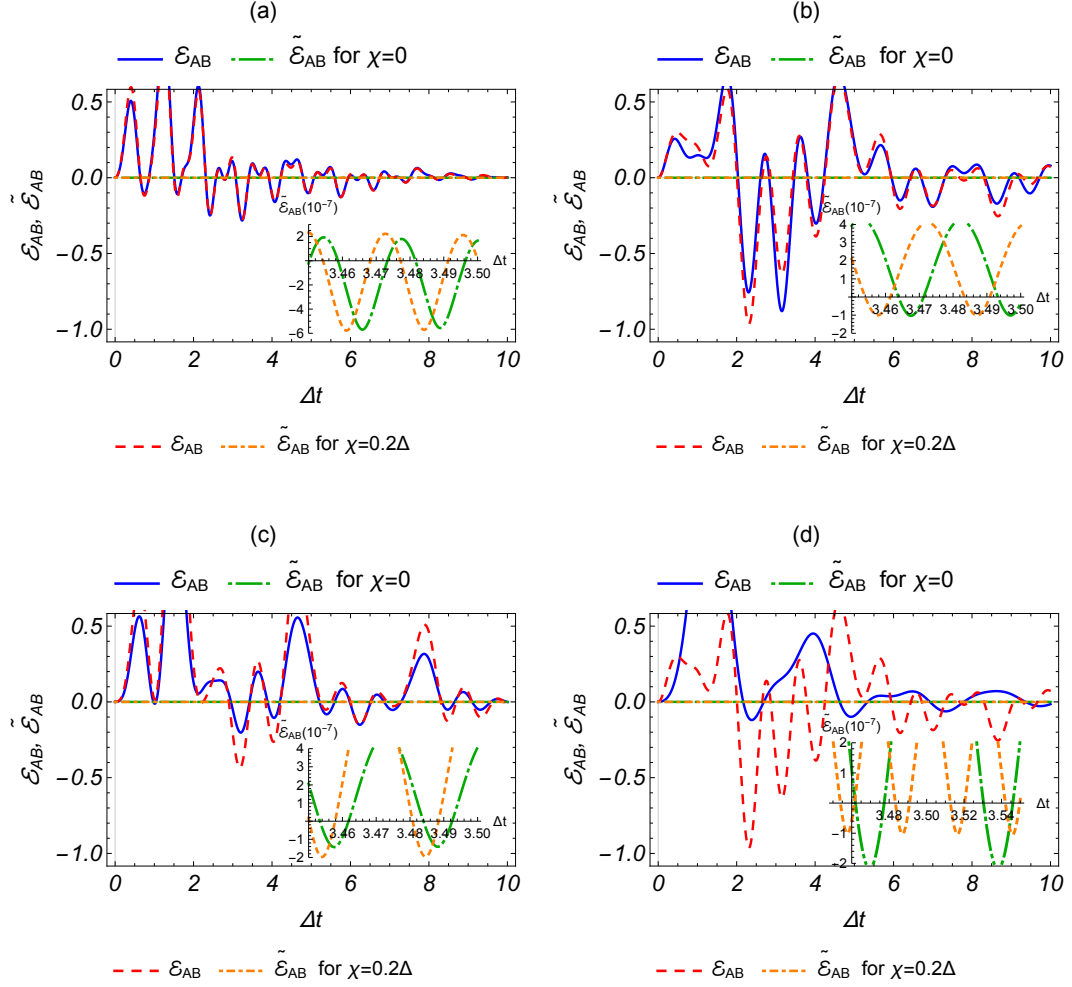


**Figure 5.9:** Hillery Zubairy criteria, as defined in Eqs. (2.51) and (2.52), plotted against the dimensionless parameter  $\Delta t$  for modes  $\hat{A}$  and  $\hat{B}$ . The figures (a), (b), (c) and (d) correspond to the AA, AN, NA and NN configurations, respectively. The negative values of the Hillery Zubairy parameters (HZPs), viz.,  $\mathcal{E}_{AB}$  and  $\tilde{\mathcal{E}}_{AB}$  provide the sufficient condition for the entanglement between the corresponding modes. The nonzero value of  $\chi$  makes HZPs more negative at certain points, and hence, enhance the entanglement between the corresponding modes.

tions. Further, it is considered that the left ensemble is driven by an external optical field which has been treated here as classical. The effects of this driving optical-field on various witnesses of single mode (e.g., squeezing, Mandel's  $Q$  parameter, antibunching) and intermodal (e.g., intermodal squeezing, antibunching, two and three mode entanglement, and steering) nonclassicality have been studied systematically. The study has yielded various interesting results which are summarized in Table 5.1.

The work illustrates how the optical-driving field may be used to control the amount of nonclassicality. In fact, it can be used to enhance the nonclassicality of the atomic ensemble modes, cavity modes and their compound modes. Specifically, it is observed that the excitation mode  $\hat{A}$  corresponding to the driven ensemble shows amplification in the witness of squeezing of its quadratures in the presence of the external field ( $\chi \neq 0$ ). Similar enhancement of the negative values of the nonclassicality witness has also been observed in the cavity photonic mode  $\hat{C}$  when the driven ensemble is placed at the Antinode of the cavity field.

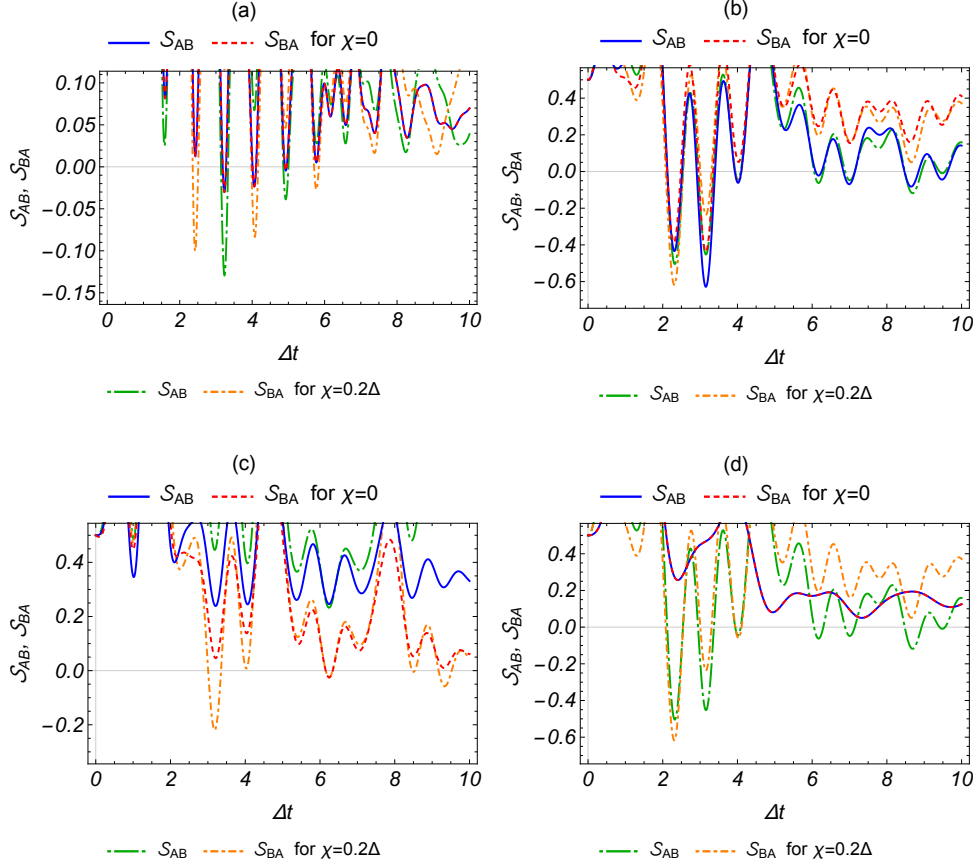


**Figure 5.10:** Steering criteria as a function of  $\Delta t$  for modes  $\hat{A}$  and  $\hat{B}$ . The figures (a), (b), (c) and (d) correspond to the AA, AN, NA and NN. Steering is confirmed if  $S_{\alpha\beta} < 0$ , for modes  $\alpha$  and  $\beta$ .

Further, the existence of entanglement which is considered to be one of the main resources for quantum information processing has been observed here using a set of sufficient criteria for inseparability. Specifically, we have used Hillery-Zubairy criterion and Duan's criterion for two-mode entanglement and a biseparability criteria for three mode scenario. Since steering can be used for one-way device independent quantum key distribution ([147] and references therein), we have also investigated the possibilities of observing steering involving various modes of the system. The investigation has not only revealed the existence of steering, but has also demonstrated its asymmetric nature.

The method adapted in this work is quite general and easy to follow. It can be extended easily to investigate the existence of nonclassicality in similar physical systems of interest, specially in a set of driven cavity systems. For example, the study can be adapted to a system where both the ensembles are driven (with the same or different driving frequencies) or to a double cavity optomechanical system [328–333]. In brief, nonclassical features of various optomechanical, driven- and non-driven cavity and optomechanics-like systems can be studied using the technique used here. Further, the present system and similar driven-cavity systems can be treated in a completely quantum mechanical manner (by considering the driving optical field as weak and hence quantum mechanical) to reveal nonclassicalities involving the mode(s) of the driving field(s). Such investigations are expected to yield various types of nonclassicality in different physical systems that can be realized with the present technology and thus provide a wider choice of systems (to experimentalists) that can be used to build quantum devices that exploit the true power of the quantum world by producing and manipulating nonclassical states.



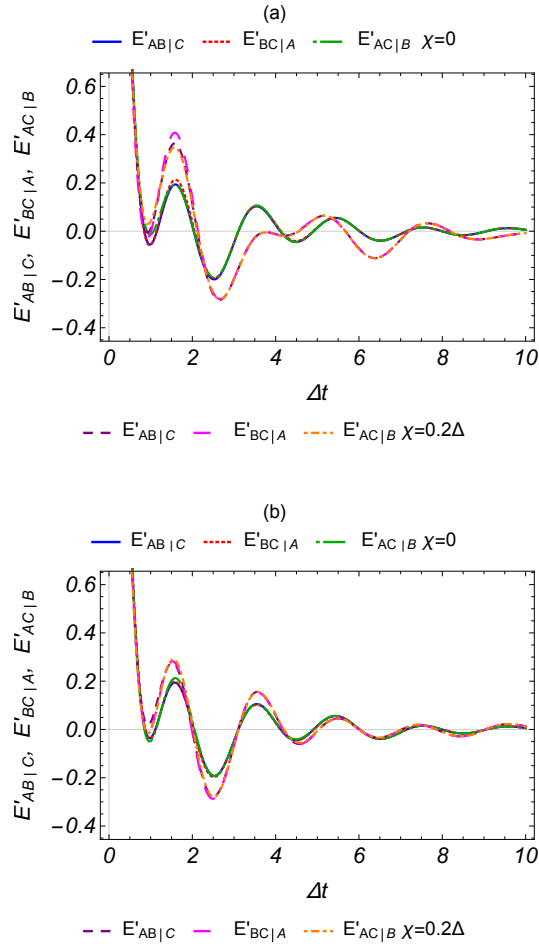


**Figure 5.11:** Biseparability criteria as a function of  $\Delta t$ . Top and bottom panels correspond to AN and NA configurations, respectively. The nonseparability of modes  $\alpha$ ,  $\beta$  and  $\gamma$  is implied by the satisfaction of either or both of the inequalities  $E_{\alpha\beta|\gamma} < 0$  and  $E'_{\alpha\beta|\gamma} < 0$ .

**Table 5.1:** Various witnesses of nonclassicality that are investigated for different configurations, both in the absence as well as in the presence of external field characterized by  $\chi$ . Here, a tick indicates the presence of a nonclassical feature characterized by the nonclassicality witness mentioned in the first column of the same row, while a cross is the indicator of failure in the detection of that nonclassicality feature. It clearly emerges that the AA configuration is more suited for observing various facets of nonclassicality in the system.

Witnesses of nonclassicality	AN configuration		NA configuration		AA configuration		NN configuration	
	$\chi = 0$	$\chi = 0.2$	$\chi = 0$	$\chi = 0.2$	$\chi = 0$	$\chi = 0.2$	$\chi = 0$	$\chi = 0.2$
Mandel parameter	✓ (A, C)	✓ (B, C)	✓ (A, C)	✓ (B, C)	✓ (A, C)	✓ (B, C)	✓ (A, C)	✓ (A,B,C)
Singlemode Squeezing	✓ (A, C)	✓ (B, C)	✓ (A, A)	✓ (B, A)	✓ (A, A)	✓ (B, A)	✓ (A, A)	✓ (B, A)
Intermodal Squeezing	✓ (AB, AC)	✓ (AB, AC)	✓ (AB, AC)	✓ (AB, AC)	✓ (AB, AC)	✓ (AB, AC)	✓ (AB, AC)	✓ (AB, AC)
Hillery Zubairy criterion ( $\mathcal{E}$ )	✓ (AB, AC)	✓ (AB, AC)	✓ (AB, AC)	✓ (AB, AC)	✓ (AB, AC)	✓ (AB, AC)	✓ (AB, AC)	✓ (AB, AC)
Hillery Zubairy criterion ( $\tilde{\mathcal{E}}$ )	✓ (AB, AC)	✓ (AB, AC)	✓ (AB, AC)	✓ (AB, AC)	✓ (AB, AC)	✓ (AB, AC)	✓ (AB, AC)	✓ (AB, AC)
Duan criterion	✓ (AB, AC)	✓ (AB, AC)	✓ (AB, AC)	✓ (AB, AC)	✓ (AB, AC)	✓ (AB, AC)	✓ (AB, AC)	✓ (AB, AC)
Biseparability criterion (E)	✓ (AB C, AC B)	✓ (AB C, AC B)	✗ (AB C, AC B)	✗ (AB C, AC B)	✓ (AB C, AC B)	✓ (AB C, AC B)	✓ (AB C, AC B)	✓ (AB C, AC B)
Biseparability criterion ( $E'$ )	✓ (AB C, AC B)	✓ (AB C, AC B)	✓ (AB C, AC B)	✓ (AB C, AC B)	✓ (AB C, AC B)	✓ (AB C, AC B)	✓ (AB C, AC B)	✓ (AB C, AC B)
Single mode antibunching	✓ (A, C)	✓ (B, C)	✓ (A, C)	✓ (B, C)	✓ (A, C)	✓ (B, C)	✓ (A, C)	✓ (A,B,C)
Intermodal antibunching	✓ (AB, AC)	✓ (AB, AC)	✓ (AB, AC)	✓ (AB, AC)	✓ (AB, AC)	✓ (AB, AC)	✓ (AB, AC)	✓ (AB, AC)
Steering	✓ (AB,BA, AC, CA)	✓ (AB,BA, AC, CA)	✗ (AB,BA, AC, CA)	✗ (AB,BA, AC, CA)	✓ (AB,BA, AC, CA)	✓ (AB,BA, AC, CA)	✗ (AB,BA, AC, CA)	✓ (AB,BA, AC, CA)